Late Paleozoic deformation and exhumation in the Sierras Pampeanas (Argentina): $^{40}Ar/^{39}Ar$-feldspar dating constraints

Stefan Löbens, Sebastián Oriolo, Jeff Benowitz, Klaus Wemmer, Paul Layer & Siegfried Siegesmund

International Journal of Earth Sciences
GR Geologische Rundschau

ISSN 1437-3254
Volume 106
Number 6

Int J Earth Sci (Geol Rundsch) (2017)
106:1991-2003
DOI 10.1007/s00531-016-1403-3

Springer

Int J Earth Sci (Geol Rundsch) (2017) 106:1991–2003
DOI 10.1007/s00531-016-1403-3

ORIGINAL PAPER

Late Paleozoic deformation and exhumation in the Sierras Pampeanas (Argentina): $^{40}Ar/^{39}Ar$-feldspar dating constraints

Stefan Löbens[1] · Sebastián Oriolo[1] · Jeff Benowitz[2] · Klaus Wemmer[1] · Paul Layer[2] · Siegfried Siegesmund[1]

Received: 20 March 2016 / Accepted: 18 September 2016 / Published online: 28 September 2016

Abstract Systematic $^{40}Ar/^{39}Ar$ feldspar data obtained from the Sierras Pampeanas are presented, filling the gap between available high- (>~300 °C) and low-temperature (<~150 °C) thermochronological data. Results show Silurian–Devonian exhumation related to the late stages of the Famatinian/Ocloyic Orogeny for the Sierra de Pocho and the Sierra de Pie de Palo regions, whereas the Sierras de San Luis and the Sierra de Comechingones regions record exhumation during the Carboniferous. Comparison between new and available data points to a Carboniferous tectonic event in the Sierras Pampeanas, which represents a key period to constrain the early evolution of the proto-Andean margin of Gondwana. This event was probably transtensional and played a major role during the evolution of the Paganzo Basin as well as during the emplacement of alkaline magmatism in the retroarc.

Keywords Carboniferous · Paganzo Basin · Andean foreland · Pampean flat-slab segment · Crustal exhumation

Electronic supplementary material The online version of this article (doi:10.1007/s00531-016-1403-3) contains supplementary material, which is available to authorized users.

Stefan Löbens
stefan.loebens@geo.uni-goettingen.de

1 Geoscience Centre, University of Göttingen, Goldschmidtstr. 3, 37077 Göttingen, Germany

2 Department of Geology and Geophysics, University of Alaska, 900 Yukon Drive, Fairbanks, AK 99775, USA

Introduction

Argon diffusion in feldspar has been widely applied to constrain the cooling and exhumation history of magmatic and metamorphic rocks (e.g., Burgess et al. 1992; Meert et al. 2001; Streepey et al. 2002; Cassata et al. 2009). It has been also used to date sub-greenschist events as well as authigenic growth of feldspars (e.g., Spötl et al. 1998; McLaren and Dunlap 2006; Mark et al. 2008; Mortimer et al. 2012). The closure temperature of this geochronological system is, however, a matter of discussion. Instead of having a single closure temperature (Dodson 1973), feldspars present multiple diffusion domains that can be potentially useful to reconstruct more complex cooling histories (Lovera et al. 1989; Burgess et al. 1992; Spötl et al. 1998; Sherlock et al. 2005; Mark et al. 2008; Benowitz et al. 2011, 2012, 2014). Hence, $^{40}Ar/^{39}Ar$ feldspar methods constitute an important tool to fill the gap between high- and low-temperature thermochronometers between approximately 300–150 °C (McDougall and Harrison 1999; Streepey et al. 2002; Cassata et al. 2009), providing powerful insights into thermal evolution of complex tectonic settings like the Sierras Pampeanas in Argentina.

The Sierras Pampeanas constitute a morphotectonic unit, which is located in the Andean foreland of the Pampean flat-slab segment between 27°S and 33°S (Fig. 1). It is made up of mostly magmatic and metamorphic rocks of late Proterozoic-Paleozoic ages (e.g.; Caminos 1979; Gordillo and Lencinas 1979; Sims et al. 1998; Casquet et al. 2001; Steenken et al. 2006; Siegesmund et al. 2010). During the late Devonian, the collision of the Chilenia microcontinent to the west of the Sierras Pampeanas gave rise to the Chanic/Achalian Orogeny (e.g., Sims et al. 1998; Steenken et al. 2010; Willner et al. 2011), which was succeeded by subduction along the proto-Andean margin.

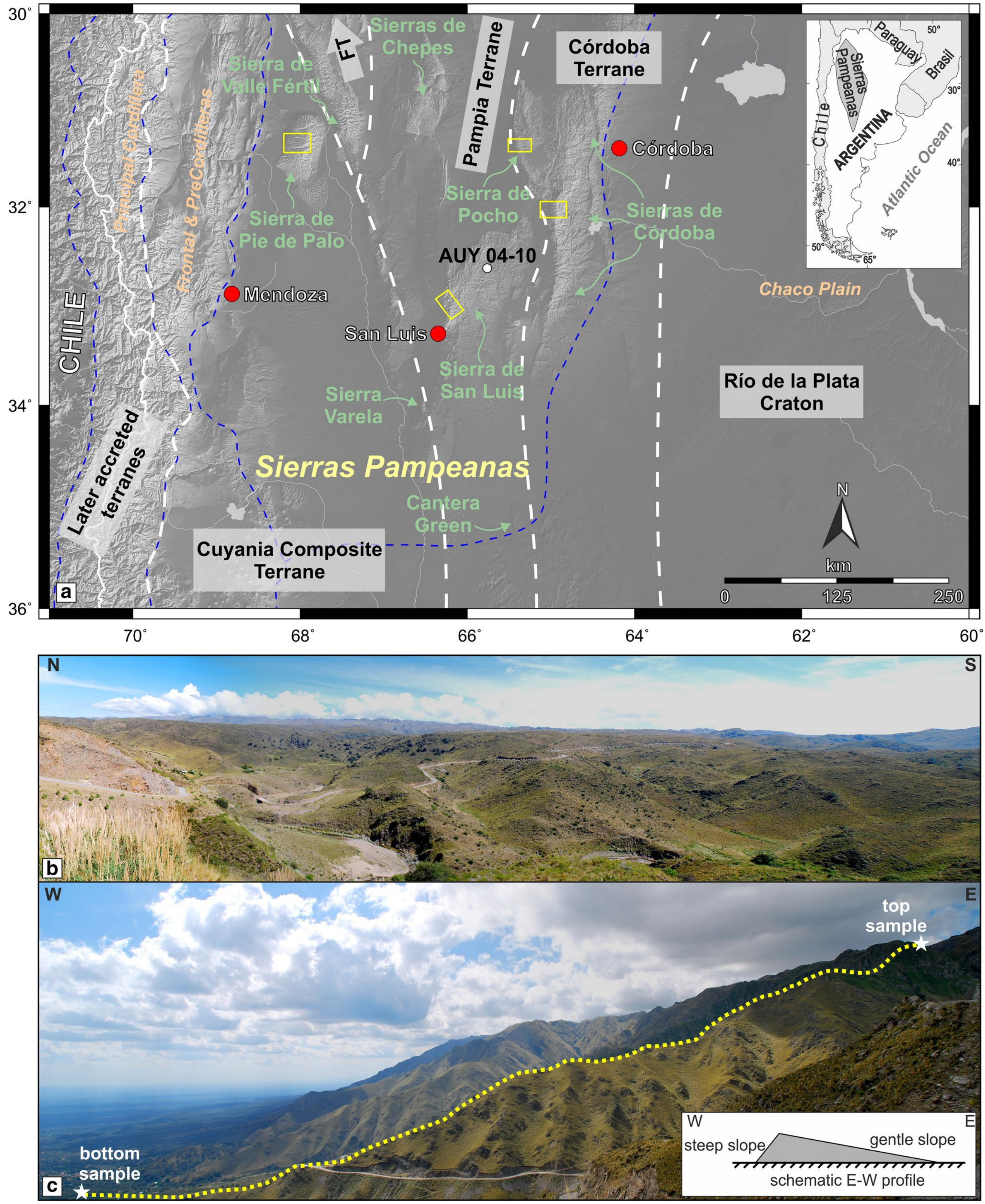
30°
32°
34°
36°
70°
68°
66°
64°
62°
60°
Sierras de Chepes
FT
Sierra de Valle Fértil
Pampia Terrane
Córdoba Terrane
Córdoba
Principal Cordillera
Frontal & PreCordilleras
Sierra de Pie de Palo
Sierra de Pocho
Sierras de Córdoba
AUY 04-10
Mendoza
San Luis
CHILE
Sierra de San Luis
Sierra Varela
Chaco Plain
Río de la Plata Craton
Later accreted terranes
Sierras Pampeanas
Cantera Green
Cuyania Composite Terrane
N
km
0
125
250
a
Chile
Sierras Pampeanas
Paraguay
Brasil
ARGENTINA
Atlantic Ocean
50°
30°
40°
50°
65°
N
S
b
W
E
top sample
bottom sample
c
W
E
steep slope
gentle slope
schematic E-W profile

◂**Fig. 1** Overview of the study area. **a** SRTM-3 model showing the different morphotectonic provinces (*sandy* and *yellow font*) separated by the *blue dashed line* (after Hilley and Coutand 2010), the different terranes (*FT* Famatinia Terrane) accreted during the different cycles of the Brasiliano Orogeny (*white dashed lines* mark the suture zones; after Vujovich and Ramos 1999; Leal et al. 2003; Rapela et al. 2007; Varela et al. 2011), and the different ranges of the Sierras Pampeans (*greenish font*). Beside the *white point* (AUY 04-10), investigated profiles are marked by the *yellow rectangles*. The *inset* in the *upper right* shows the area of the Sierras Pampeanas on the South American Continent. **b**, **c** The gentle dipping eastern slope and the steep western slope generally characterising the mountain ranges of the Eastern Sierras Pampeanas (e.g. the Sierra de Comechingones), respectively. This is also schematically exhibited in the lower right (modified from Löbens et al. 2011). The *white stars* in (**c**) mark the samples taken along the profiles indicated by the *yellow rectangles* in (**a**)

Nevertheless, the Carboniferous evolution of the Sierras Pampeanas is a matter of ongoing debate. Martino (2003), Siegesmund et al. (2004) and Steenken et al. (2010) argued that the area was characterised by a compressional/transpressional regime until the very early Carboniferous, whereas other authors (Chernicoff and Zappettini 2007; Alasino et al. 2012; Dahlquist et al. 2014) proposed the existence of an extensional/transtensional setting. The latter is further supported by the Carboniferous–Permian sediment record of the Paganzo Basin in the Sierras Pampeanas, which was linked to the evolution of pull-apart basins during dextral transtension (Fernández Seveso and Tankard 1995; Simpson et al. 2001). However, except of the work from Jordan et al. (1989), available data constraining the thermal evolution of the Sierras Pampeanas during this period are scarce.

This contribution presents systematic $^{40}Ar/^{39}Ar$ feldspar data for this region, which allow filling the gap between available high- and low-temperature thermochronological data (e.g. Jordan et al. 1989; Siegesmund et al. 2010; Steenken et al. 2010; Löbens et al. 2011, 2013a, b; Bense et al. 2013; Enkelmann et al. 2014; Garber et al. 2014). Moreover, these data provide constraints on the differential thermal histories in both the Western and Eastern Sierras Pampeanas, particularly related to the late Paleozoic exhumation and tectonic evolution.

Geological setting

In the late Proterozoic and middle Paleozoic, different allochthonous and parautochthonous terranes were accreted to the southwestern margin of the Río de la Plata Craton during the Pampean, Famatinian, and Achalian orogenies, which in part led to the formation of the Sierras Pampeanas (Ramos 1988; Rapela et al. 1998, 2007; Sims et al. 1998; Steenken et al. 2006, 2010; Willner et al. 2011). These ranges represent tectonic blocks, which are mainly characterised by crystalline basement and crop out in the Andean foreland (González Bonorino 1950; Caminos 1979; Gordillo and Lencinas 1979). Although ductile deformation associated with the early tectonometamorphic evolution of the Sierras Pampeanas is considered to be completed by the late Devonian-early Carboniferous (Fig. 1; Ramos 1988; Simpson et al. 2001; Ramos et al. 2002; Martino 2003; Steenken et al. 2004; Miller and Söllner 2005), exhumation and brittle deformation persisted until the Holocene (e.g. Jordan et al. 1989; Costa and Vita Finzi 1996; Simpson et al. 2001; Wemmer et al. 2011; Löbens et al. 2011, 2013a, b; Richardson et al. 2012; Bense et al. 2013, 2014; Siame et al. 2015).

During the late Paleozoic, calc–alkaline and alkaline magmatism was recorded in the Western and Eastern Sierras Pampeanas, respectively (Dahlquist et al. 2010, 2014, 2015; Alasino et al. 2012). Although the local tectonic setting (compression/extension) of this period of magmatism is still controversial, it was related to the subduction along the proto-Andean margin (Pankhurst and Rapela 1998). Likewise, Carboniferous–Permian sedimentation is recorded in the Paganzo Group, which constitutes the extensional retroarc Paganzo basin (Limarino and Spalletti 2006; Limarino et al. 2006). Subsequent inversion of this basin took place during flat-slab subduction during the late Permian San Rafael Orogeny (Geuna et al. 2010; Kleiman and Japas 2009). The first Mesozoic extensional reactivation of terrane boundaries occurred in the Late Triassic to Early Jurassic generating sedimentation of non-marine sediments in localised depocentres, which are characterised by NNW-trending basins (Criado Roque et al. 1981; Aceñolaza and Toselli 1988; Ramos et al. 2002). Extension during the early Cretaceous is associated with the opening of the southern Atlantic Ocean (Schmidt et al. 1995; Rossello and Mozetic 1999), developing major but narrow rift basins along the margins of the Pampia terrane.

Andean uplift was mostly related to the compression due to the subduction of the aseismic Juan Fernández Ridge that gave rise to Miocene flat-slab subduction (Pilger 1984; Gutscher et al. 2000; Yáñez et al. 2001). Deformation and exhumation of the Sierras Pampeanas during this period was mainly controlled by the orientation of the older late Proterozoic to Paleozoic structures, resulting in a dominance of east-dipping structures, which are morphologically expressed by a distinct asymmetry of the Pampean basement blocks, generally showing a steep dipping western slope and a gentle dipping eastern slope (Fig. 1b, c; González Bonorino 1950; Gordillo and Lencinas 1979; Criado Roque et al. 1981; González Diaz 1981; Jordan and Allmendinger 1986; Introcaso et al. 1987; Costa and Vita Finzi 1996; Ramos et al. 2002; Martino 2003). However, whether flattening of the Nazca Plate subduction angle caused the total uplift and exhumation of the

Table 1 Compilation of ages obtained by $^{40}Ar/^{39}Ar$ feldspar dating

Sample name	Long (°) Lat (°)	Elevation (m)	Integrated age (Ma)	Plateau age (Ma)	Error (Ma)	Isochron age (Ma)	Error (Ma)	Age span (Ma)	Error (Ma)
APM 15–08	−65.029333 −32.047000	831	–	315.0	10.0	–	–	–	–
AUY 04–10	−65.759747 −32.598398	1121	327.5	–	1.2	–	–	320.3–331.0	1.1/1.4
APM 34–08	−66.203667 −33.004833	2085	308.2	–	1.1	–	–	302.8–319.4	2.1/2.2
APM 48–08	−66.243500 −32.976333	1269	325.8	–	1.2	–	–	313.0–330.6	1.6/2.0
APM 54–08	−65.296333 −31.375000	1075	–	418.9	1.8	421.6	3.1	–	–
AUY 56–10	−67.929343 −31.311922	3133	420.7	–	1.5	–	–	–	–

Due to the generally homogenous radiogenic content of the plateau release, isochron age determinations were not possible for most samples

Sierras Pampeanas has been a matter of discussion over the last decades (e.g. Jordan et al. 1983, 1989; Coughlin et al. 1998; Kay and Abbruzzi 1996; Ramos et al. 2002; Löbens et al. 2011, 2013a; Bense et al. 2013; Dávila and Carter 2013).

Methodology

Granitoid and gneiss rock samples from different mountain ranges in the Sierras Pampeanas were collected along elevation transects, in order to better evaluate the thermal and inferred exhumation history of these ranges using $^{40}Ar/^{39}Ar$-dating of feldspars. For this purpose, at least, one sample from the top and the bottom, respectively, is necessary to receive a robust dataset (Fig. 1a, c).

For $^{40}Ar/^{39}Ar$ analysis, samples were crushed, sieved, washed and hand-picked for plagioclase and potassium feldspar mineral phases at the Geochronology laboratory at the University of Alaska Fairbanks (Fig. 1; Table 1). The monitor mineral MMhb-1 (Samson and Alexander 1987) with an age of 513.9 Ma (Lanphere and Dalrymple 2000) was used to monitor neutron flux (and calculate the irradiation parameter, J). The samples and standards were wrapped in aluminium foil and loaded into aluminium cans of 2.5 cm diameter and 6 cm height. The samples were irradiated in position 5c of the uranium enriched research reactor of McMaster University in Hamilton, Ontario, Canada, for 20 megawatt-hours.

Upon their return from the reactor, the samples and monitors were loaded into 2-mm-diameter holes in a copper tray that was then loaded in an ultra-high vacuum extraction line. The monitors were fused, and samples heated, using a 6-watt argon-ion laser following the technique described in York et al. (1981), Layer et al. (1987) and Layer (2000). Argon purification was achieved using a liquid nitrogen cold trap and a SAES Zr–Al getter at 400 °C. The samples were analysed in a VG-3600 mass spectrometer at the Geophysical Institute, University of Alaska Fairbanks. The argon isotopes measured were corrected for system blank and mass discrimination, as well as calcium, potassium and chlorine interference reactions following procedures outlined in McDougall and Harrison (1999). System blanks generally were 2×10^{-16} mol ^{40}Ar and 2×10^{-18} mol ^{36}Ar which are 10–50 times smaller than fraction volumes. Mass discrimination was monitored by running both calibrated air shots and a zero-age glass sample. These measurements were made on a weekly to monthly basis to check for changes in mass discrimination.

A bulk furnace-run of sample AUY-56-10 consisting of 4K-feldspar crystals was reloaded in an aluminium packet and into the finger of a glass storage tree. It was then attached to the top of a Modifications Ltd. low-blank furnace connected online to the mass spectrometer. The sample was step-heated after being dropped into the furnace tantalum crucible. The furnace is controlled using a Eurotherm thyristor and controller. Temperature was monitored by means of a thermocouple positioned in a pit at the base of the crucible and a maximum temperature in excess of 1600 °C is achievable. A molybdenum liner was not used to (a) increase accuracy of the diffusion experiment recorded temperature by lessening the distance from the thermocouple to the degassing sample, (b) lessen thermal mass of the unit to decrease heating time and decrease cooling off time and (c) cost considerations.

The furnace was calibrated by both the colour temperature correlation assuming a black body (Davis 1931), by the temperature aluminium foil melts at (660 °C), and collaborated by the breakdown of volume diffusion behaviour in K-feldspar above 1150 °C (Lovera et al. 1991) demonstrated by irregular higher temperature age spectra. Temperature was recorded every 30 s and averaged to mitigate and take into account heat up time, cool off time and any slight over shot of set temperature. Recorded temperature is estimated to have an error of ±5 °C with a limited effect on thermal models based on numerous diffusion experiments on the same sample (Lovera et al. 2002).

Approximately 31 duplicated isothermal step-heating schedules were conducted on the K-spar separates in order to retrieve ^{39}Ar diffusion characteristics, to apply diffusion models, and to calculate model thermal histories (Harrison et al. 1994; Lovera et al. 1993). About three high-temperature step-heats (>~1150) were run to fully degas the furnace before the next analysis and were not input for MDD thermochronology. Twelve-minute blanks were run at room temperature (cold blank), ~588 and ~980 °C. Typical full system cold 12-min furnace blank values were generally 3×10^{-15} mol ^{40}Ar, 1×10^{-18} mol ^{39}Ar, 1×10^{-17} mol ^{38}Ar and 1×10^{-17} mol ^{36}Ar. Blanks at ~588 and ~980 °C were generally the same at 5×10^{-15} mol ^{40}Ar, 3×10^{-18} mol ^{39}Ar, 1×10^{-17} mol ^{38}Ar and 2×10^{-17} mol ^{36}Ar.

A summary of all the ^{40}Ar/^{39}Ar results is given in Table 1, with all ages quoted to the ±1 sigma level and calculated using the constants of Steiger and Jaeger (1977). The integrated age is the age given by the total gas measured and is equivalent to a potassium–argon (K–Ar) age. The spectrum provides a plateau age if three or more consecutive gas fractions represent at least 50 % of the total gas release and are within two standard deviations of each other (mean square-weighted deviation less than ~2.5).

Results and methodical interpretation

Just six out of 14 samples show reliable ages. Either the plagioclase or potassium feldspar-content of the other samples was too less for analyses or the K-content of the separates was limited, resulting in geologically meaningless ages that were thus rejected.

^{40}Ar/^{39}Ar ages are assigned to plagioclase or potassium feldspar mineral phases based on the Ca/K ratio >1 and the Ca/K ratio <1, respectively. The resulting ages of the samples from the Sierra de Pocho and Sierra de Pie de Palo as well as the Sierra de Comechingones and the Sierra de San Luis range between the Silurian-Devonian and the Carboniferous, respectively (Fig. 2; Table 1, supplementary material).

Sample APM 54-08 from the Sierra de Pocho was determined to be of the plagioclase mineral phase based on the Ca/K ratio being >1 for the steps chosen for the plateau age determination and shows Silurian ^{40}Ar/^{39}Ar ages. Since the integrated age (428.8 ± 1.9 Ma), the plateau age (418.9 ± 1.8 Ma) and the isochron age (421.6 ± 3.1 Ma) are comparable, the plateau age of 418.9 ± 1.8 Ma is preferred for this sample due to the higher precision compared to the isochron age.

Sample AUY 56-10 from the Sierra de Pie de Palo was determined to be of the potassium feldspar phase based on having a Ca/K ratio <1 and produced an integrated ^{40}Ar/^{39}Ar age of 420.7 ± 1.5 Ma (Silurian; Fig. 2; Table 1, supplementary material). The integrated age (420.7 ± 1.5 Ma) for unaltered potassium feldspar samples can reflect the complete cooling history of a sample that cools quickly from ~350 to ~150 °C (e.g. Benowitz et al. 2012). A down-stepping age spectra may reflect a more complex thermal history as is the case of this sample which is also reflected in its modelled thermal history (Fig. 3), which was produced by using the MDD software of Lovera et al. (2002). The sample cooled from 434.5 ± 1.6 Ma (maximum age steps used in thermal model) to ~150 °C by ~390 Ma (approx. 4.5 °C/Ma), where the sample sat till closure of the feldspar system (Fig. 3). The last ~5 % of the gas release had an unusual step down-stepping age pattern, which might reflect loss to alteration of continued thermally controlled Ar loss.

Sample APM 15-08 was determined to be of the plagioclase phase based on having a Ca/K ratio >1. ^{40}Ar/^{39}Ar-plagioclase dating of the sample APM 15-08 from the Sierra de Comechingones (Sierras de Córdoba) shows Carboniferous ages. The integrated age (318.7 ± 11.8 Ma) and the plateau age (315.0 ± 10.0 Ma) are within error. The plateau age of 315.0 ± 10.0 Ma is preferred because of the anomalously old ages produced during the high-temperature step-releases. These steps are also associated with a low K, high Ca phase of the mineral reflecting unreliable age dating for these components of the step-heat. An isochron age determination was not possible because of the generally homogenous radiogenic content of the plateau release.

Samples AUY 04-10, APM 34-08, and APM 48-08 were determined to be of the potassium feldspar phase based on a Ca/K ratio <1. The ^{40}Ar/^{39}Ar age determinations of potassium feldspar of the samples from the Sierra de San Luis (AUY 04-10, APM 34-08, and APM 48-08) show a slightly down-stepping age spectra; thus, a maximum/minimum age determination approach for these samples was selected. Additionally, the first step age of sample AUY 04-10 is likely affected by excess argon demonstrated by the high Cl/K ratio (supplementary material). Overall, the samples from the Sierra de San Luis show minimum ($KFAT_{min}$) and maximum ($KFAT_{max}$) ages lying in the Carboniferous. Particularly, the $KFAT_{max}$ and $KFAT_{min}$ ages of AUY 04-10 from the Las Chacras Batholith and of APM 48-08 from the bottom of the investigated transect are similar, ranging between 331.0 ± 1.0 and 330.6 ± 2.0 Ma as well as between 320.3 ± 1.1 and 313.0 ± 1.6 Ma, respectively (Table 1). APM 34-08 (the uppermost sample from the

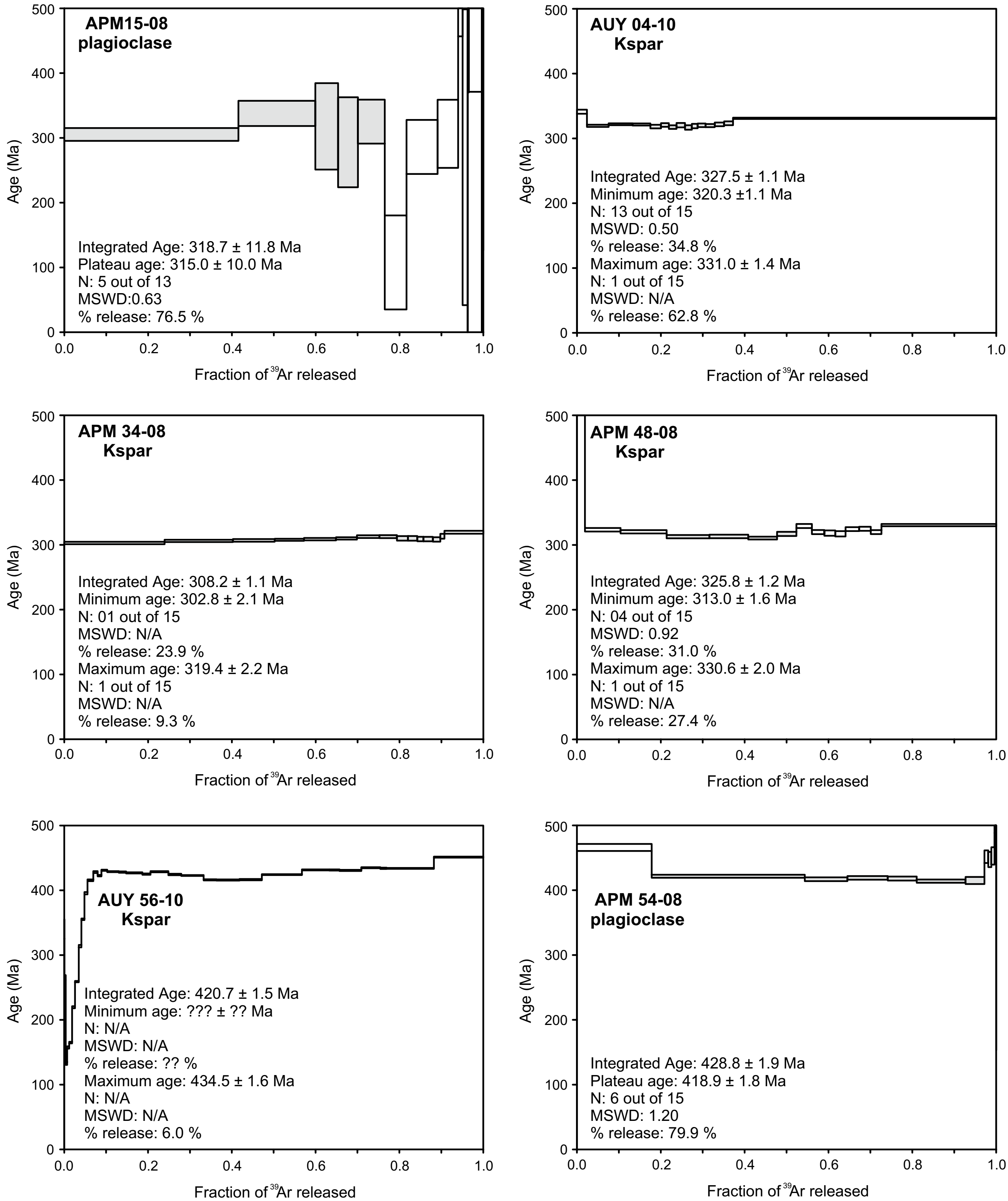

Fig. 2 $^{40}Ar/^{39}Ar$ age spectra of the different samples. Details are mentioned in the text

transect) is characterised by ages between 319.4 ± 2.2 and 302.8 ± 2.1 Ma, thus being younger than the former mentioned samples.

Discussion

Thermal evolution

The obtained age for the Sierra de Pocho (418.9 ± 1.8 Ma) is in good agreement with available higher temperature K–Ar biotite (ca. 433–430 Ma; Steenken et al. 2010) and lower temperature (U–Th)/He zircon data (ca. 308 Ma; Bense et al. 2013). Based on K–Ar muscovite data, Steenken et al. (2010) constrained deformation along the Pachango shear zone in the southern Sierra de Pocho at ca. 420 Ma, which is equivalent to the data presented herein. Consequently, exhumation and cooling below 225 °C (plagioclase $^{40}Ar/^{39}Ar$ results this study) of the Sierra de Pocho seems to be related to the latest stages of the Famatinian deformation during the late Silurian (Fig. 3).

Likewise, new data for the Sierra de Pie de Palo (434.5 ± 1.6 Ma $KFAT_{max}$; ~390 Ma $KFAT_{min}$) are younger than $^{40}Ar/^{39}Ar$ hornblende and muscovite ages (441 ± 16 and 436 ± 4 Ma, respectively) reported by Mulcahy et al. (2011) for the Central Complex in the hanging wall of the Duraznos Shear Zone. On the other hand, $^{40}Ar/^{39}Ar$ muscovite ages between ca. 432–394 Ma were obtained for the Central Complex (Ramos et al. 1998), suggesting differential cooling due to segmentation associated with other shear zones (Garber et al. 2014). Garber et al. (2014) reported both $^{40}Ar/^{39}Ar$ hornblende and muscovite ages of ca. 405–400 Ma near the Bajo Pequeño shear zone, indicating progressive strain localisation along this shear zone and ductile deformation up to ~400 Ma. Likewise, the collision of the Chilenia microcontinent was constrained at ~390 Ma (Willner et al. 2011). Therefore, exhumation of the Sierra de Pie de Palo probably resulted mostly from the docking of the Cuyania terrane to the Gondwana margin during the Ordovician Ocloyic Orogeny as indicated by Ramos et al. (1998), and conditions below ~150 °C were attained almost contemporaneously with the onset of the collision of Chilenia (Fig. 3).

An $^{40}Ar/^{39}Ar$ K-feldspar analysis of a single sample from the Sierras de Córdoba (Jordan et al. 1989) produced similar Carboniferous age results and age spectrum as new $^{40}Ar/^{39}Ar$ K-feldspar data (Fig. 4). Jordan et al. (1989) interpreted their results to reflect slow cooling between the time interval from ~320 to ~260 Ma. This pioneering work was carried out before there was a paradigm shift in the understanding of Ar diffusion domains in K-feldspar (Lovera et al. 1991). Hence, $^{40}Ar/^{39}Ar$ K-feldspar results from Jordan et al. (1989) are reconsidered in the context of the multi-diffusion domain approach and recalculated, providing a plateau age of 319.2 ± 1.7 Ma (62 % of non-discounted ^{39}Ar release). Based on the shape of the age spectrum, it is inferred that this sample cooled rapid at this time through the majority of the closure temperature (Tc) for $^{40}Ar/^{39}Ar$ in K-feldspar providing similar cooling paths such as samples AUY 04-10 (Fig. 4).

Furthermore, the onset of deformation under conditions below brittle–ductile transition conditions is constrained at ~345–335 Ma by $^{40}Ar/^{39}Ar$ biotite ultramylonite data for the Sierra de Comechingones (Whitmeyer 2008). This is further supported by K–Ar fault gouge ages indicating brittle deformation between 340 and 300 Ma (Löbens et al. 2011). Consequently, Carboniferous exhumation of the Sierra de Comechingones was clearly related to active deformation.

In a similar way, all $^{40}Ar/^{39}Ar$ feldspar data from the Sierra de San Luis show Carboniferous ages (~330–300 Ma), which are significantly younger than most K–Ar muscovite ages obtained elsewhere along this range (Sims et al. 1998; Krol and Simpson 1999; Krol et al. 2000; Siegesmund et al. 2004). Only scarce K–Ar mica ages of the Las Chacras Batholith record late Devonian to Carboniferous ages (>~340 Ma; Siegesmund et al. 2004), whereas zircons from basement units yield late Pennsylvanian (U–Th)/He ages (Bense et al. 2013). Therefore, the Sierra de San Luis underwent cooling below brittle–ductile transition conditions during the upper Carboniferous, which was associated with active deformation based on coeval K–Ar illite fine-fraction ages between ~330 and ~290 Ma (Wemmer et al. 2011).

Implications for the late Paleozoic evolution

New systematic $^{40}Ar/^{39}Ar$ feldspar data as well as recalculation of $^{40}Ar/^{39}Ar$ K-feldspar data from Jordan et al. (1989) point to a differential cooling and exhumation of the blocks that constitute the Sierras Pampeanas during the late Paleozoic, supporting previous hypothesis of Jordan et al. (1989) indicating that the Sierras Pampeanas was a mountainous area during the deposition of the Paganzo sediments and thermochronological data presented by Löbens et al. (2011, 2013a, b) and Bense et al. (2013, 2014). Particularly, $^{40}Ar/^{39}Ar$ feldspar data indicate that the Sierra de Pie de Palo and the Sierra de Pocho underwent cooling below 150 °C during the Silurian-Devonian, whereas the Sierra de San Luis and the Sierra de Comechingones achieved similar conditions during the Carboniferous (Fig. 3). Silurian-Devonian exhumation was related to the last stages of the Famatinian/Ocloyic orogenic phase, but the Carboniferous regional tectonic setting of the Sierras Pampeanas demands further discussion (Wemmer et al. 2011; Bense et al. 2014).

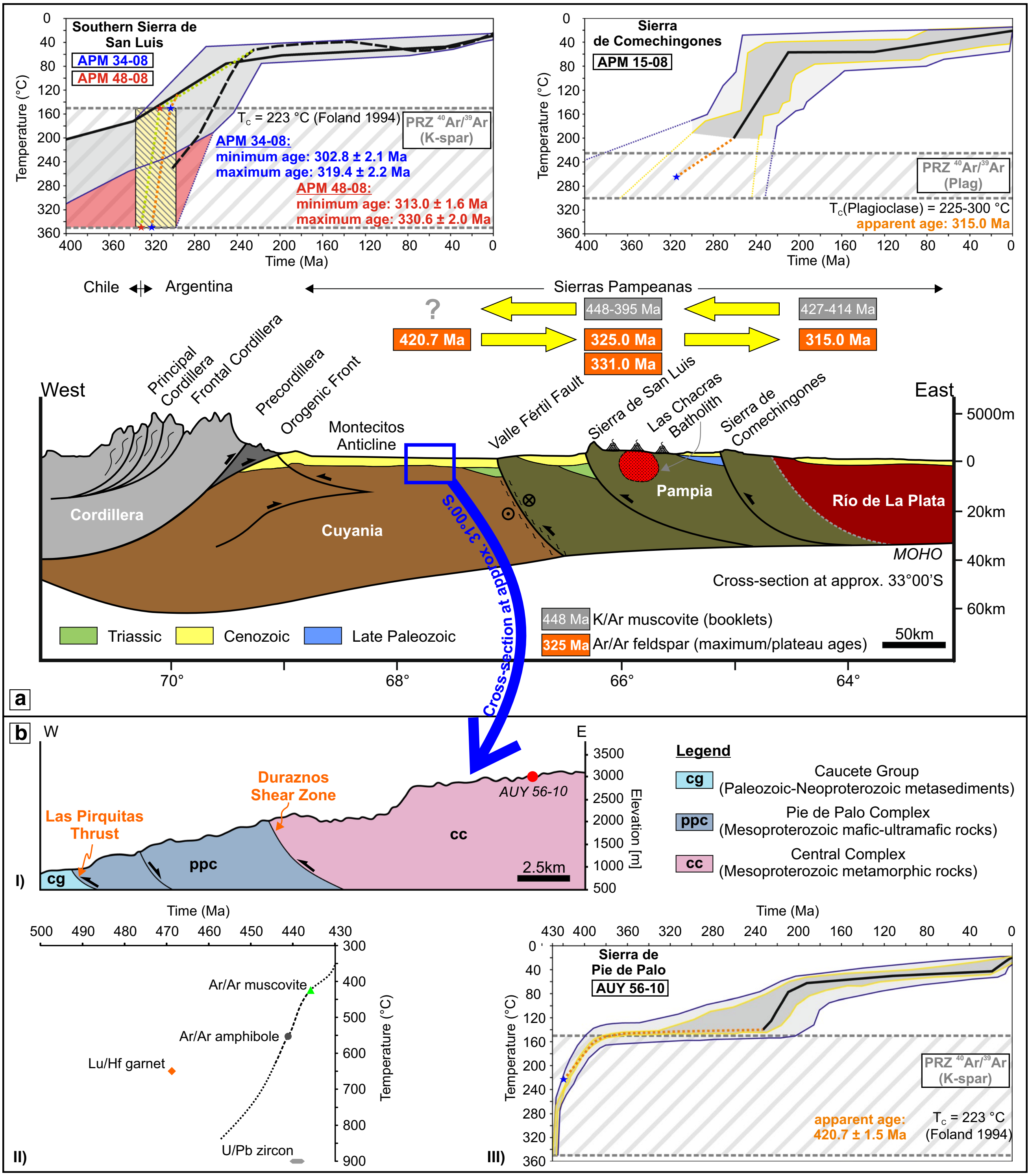

The retroarc Paganzo Basin comprises Carboniferous–Permian sedimentary sequences that reflect provenance from the basement of the Sierras Pampeanas (Net and Limarino 2006; Limarino et al. 2013; Enkelmann et al. 2014). Sedimentation began during the Upper Mississippian (331–323 Ma) and basin inversion started at ca. 260 Ma during the San Rafael Orogeny (Geuna et al. 2010; Kleiman and Japas 2009). Additionally, this basin records the Mississippian Río Blanco orogenic phase as well as intra-Carboniferous tectonic discordances

◂**Fig. 3** $^{40}Ar/^{39}Ar$ feldspar ages fill the gap between high- and low-temperature thermochronologic ages obtained for the different areas of the Eastern and Western Sierras Pampeanas. **a** schematic cross section through the Sierras Pampeanas along 33°00′ (modified after Ramos et al. 2002). The included K/Ar muscovite ages by Steenken et al. (2010) show a younging from east to west being related to the different accretional cycles of the Brasiliano Orogeny, whereas our $^{40}Ar/^{39}Ar$ feldspar ages exhibit an opposite trend, younging towards the east, similar to the trend of low temperature results presented by Löbens et al. (2011, 2013b) and Bense et al. (2014). Additionally, $^{40}Ar/^{39}Ar$ feldspar ages have been added to the cooling paths of samples from the Sierra de San Luis and the Sierra de Comechingones (Bense et al. 2014; Löbens et al. 2011), which are shown in the *upper left* and *right*, respectively. The extended paths suggest a distinct cooling in both areas during the Carboniferous. Concerning the cooling history of the Eastern Sierras Pampeanas further details are mentioned in the text. **b** Cross section of the Sierra de Pie de Palo along 31°00′ S [the position along W–E strike within the Sierras Pampeanas is indicated by the *blue rectangle* in (**a**)] showing the different tectonostratigraphic units (after Mulcahy et al. 2011 and Löbens et al. 2013b) and the location of sample AUY 56-10. In part *II* and *III* a general cooling path through the closure temperatures of different high-temperature chronometers for the Central Complex (ages obtained from Mulcahy et al. 2011; closure temperatures obtained from Harrison 1981; Foland 1994; Dahl 1997; Cherniak and Watson 2000; Harrison et al. 2009) as well as the inclusion of the modelled cooling path of the $^{40}Ar/^{39}Ar$ feldspar dating into the low-temperature cooling model from Löbens et al. (2013b) are shown. The modelled time–temperature path indicates *i* a distinct cooling during the Late Silurian and *ii* that the $^{40}Ar/^{39}Ar$ feldspar chronometer is an appropriate tool to reveal the mid-temperature (between approx. 350 and 150 °C) history of mountain ranges. Concerning the cooling history of the Western Sierras Pampeanas, further details are mentioned in the text

(Bahlburg and Breitkreuz 1991; Limarino and Spalletti 2006; Limarino et al. 2006; Gulbranson et al. 2010). Likewise, Carboniferous rapid exhumation was also reported for the Sierra de Chepes, which are comparable with tectonically active mountain ranges (Enkelmann et al. 2014).

Carboniferous deformation implied not only brittle reactivation of several basement structures but also nucleation of fault systems that cross-cut metamorphic fabrics (Simpson et al. 2001; Whitmeyer 2008; Limarino et al. 2013). Interestingly, Carboniferous polymetallic vein-type ore deposits are ubiquitously recorded in the Sierras Pampeanas (e.g. Mutti et al. 2007; Hongn et al. 2010), in which the Sierra de San Luis and Sierras de Córdoba are dominantly characterised by subvertical N- to NW-striking extensional veins (Brodtkorb et al. 1999; Mutti et al. 2007; Maffini et al. 2012; Maffini 2015). These systems have been typically interpreted as the result of strike-slip along ~N-striking structures with local areas of extension resulting from the presence of releasing bends (Mutti et al. 2007; Hongn et al. 2010). However, ~N-striking structures are sometimes mineralised (Brodtkorb et al. 1999; Mutti et al. 2007), indicating extension to some extent along these structures, thus pointing to a possible transtensional setting (Fossen and Tykoff 1998). A similar kinematic scenario can be inferred for the Paganzo Basin due to the presence of pull-apart depocentres and strike-slip deformation (Fernández Seveso and Tankard 1995; Simpson et al. 2001; Chernicoff and Zappettini 2007), whereas an extensional setting has been proposed for the Carboniferous magmatism (Dahlquist et al. 2010, 2014, 2015; Alasino et al. 2012). Therefore, retroarc sedimentation in the Paganzo Basin, emplacement of magmatism and associated mineralisations were probably controlled by transtension, although more structural and kinematic data are necessary to evaluate this hypothesis.

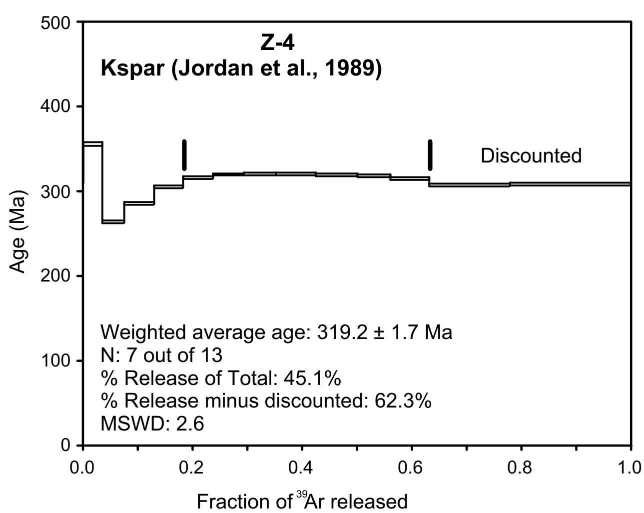

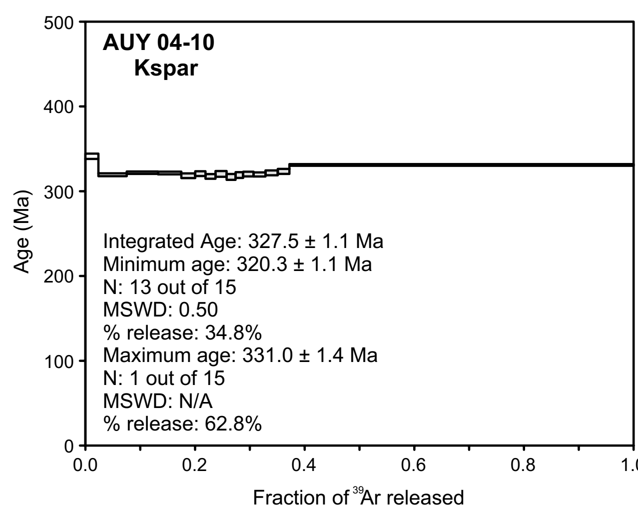

Fig. 4 Comparison of 40Ar/39Ar K-feldspar analysis of samples from the Sierras de Córdoba. On the *left side*, a recalculation of Z-4 from Jordan et al. (1989) is shown and on the *right side* the age spectra of sample AUY 04-10, achieved by applying the multi-diffusion domain approach, presented in this study. The age spectra do not show significant differences; thus, age and cooling history of these samples are similar

Conclusions

Systematic ^{40}Ar/^{39}Ar feldspar data reinforce the idea of pre-Neogene exhumation of the Sierras Pampeanas. These results show exhumation related to the Famatinian/Ocloyic Orogeny for the Sierra de Pocho and the Sierra de Pie de Palo, whereas the Sierras de San Luis and the Sierra de Comechingones record exhumation during the Carboniferous.

A review of new and available thermochronological data together with geological, structural and sedimentological evidences points to a distinct Carboniferous tectonic event in the Sierras Pampeanas, which postdates the late Devonian collisional orogeny and predates the Permian San Rafael orogenic phase. This possible transtensional event played a major role during the development and the evolution of the Paganzo Basin as well as during the emplacement of alkaline magmatism in the retroarc. Although data are still required to constrain the temporal and spatial relationships between exhumation, magmatism, sedimentation and deformation, the Carboniferous evolution of the Sierras Pampeanas constitutes a key point to constrain the early evolution of the proto-Andean margin of Gondwana.

References

Aceñolaza FG, Toselli AJ (1988) El Sistema de Famatina, Argentina: su interpretación como orógeno de margen continental activo. V Congreso Geológico Chileno 1:55–67

Alasino PH, Dahlquist JA, Pankhurst RJ, Galindo C, Casquet C, Rapela CW, Larrovere MA, Fanning CM (2012) Early Carboniferous sub- to mid-alkaline magmatism in the Eastern Sierras Pampeanas, NW Argentina: a record of crustal growth by the incorporation of mantle-derived material in an extensional setting. Gondwana Res 22:992–1008

Bahlburg H, Breitkreuz C (1991) Paleozoic evolution of active margin basins in the southern Central Andes (northwestern Argentina and northern Chile). J S Am Earth Sci 4:171–188

Benowitz J, Layer P, Armstrong P, Perry S, Haeussler P, Fitzgerald P, VanLaningham S (2011) Spatial variations in focused exhumation along a continental-scale strike-slip fault: the Denali Fault of the Eastern Alaska Range. Geosphere 7(2):455–467. doi:10.1130/GES00589.1

Benowitz J, Vansant G, Roeske S, Layer PW, Hults CP, O'Sullivan P (2012) Geochronological constraints on the Eocene to Present slip rate history of the eastern Denali Fault System. Geol Soc Am Abst Prog 44(7):634

Benowitz J, Layer PW, VanLaningham S (2014) Persistent long-term (~24 Ma) exhumation in the Eastern Alaska Range constrained by stacked thermochronology. Geological Society of London Special Volume, ^{40}Ar/^{39}Ar Dating: from Geochronology to Thermochronology, from Archaeology to Planetary Sciences

Bense F, Löbens S, Dunkl I, Wemmer K, Siegesmund S (2013) Is the exhumation of the Sierras Pampeanas only related to Neogene flat-slab subduction? Implications from a multi-thermochronological approach. J S Am Earth Sci 48:123–144

Bense F, Wemmer K, Löbens S, Siegesmund S (2014) Fault gouge analysis: K–Ar illite dating, clay mineralogy and tectonic significance—a study from the Sierras Pampeanas, Argentina. Int J Earth Sci 103:189–218

Brodtkorb MK, Fernández RR, Pezzutti N, Fernández Tasende J (1999) Yacimientos de wolframio en la zona de cizalla Río Guzmán, San Luis. In: Zappettini EO (ed) Recursos minerales de la República Argentina, vol 35. Instituto de Geología y Recursos Minerales, SEGEMAR, Anales, Buenos Aires, pp 685–687

Burgess R, Kelley SP, Parsons I, Walker FDL, Worden RH (1992) ^{40}Ar/^{39}Ar analysis of perthite microstructures and fluid inclusions in alkali feldspars from the Klokken syenite, South Greenland. Earth Planet Sci Lett 109:147–167

Caminos R (1979) Sierras Pampeanas Noroccidentales; Salta, Tucumán, Catamarca, La Rioja y San Juan. In: Turner JC (ed) Segundo Simposio de Geología Regional Argentina. Academia Nacional de Ciencias, Washington, pp 225–291

Casquet C, Baldo E, Pankhurst RJ, Rapela CW, Galindo C, Fanning CM, Saavedra J (2001) Involvement of the Argentine Precordillera terrane in the Famatinian mobile belt: U-Pb SHRIMP and metamorphic evidence from the Sierra de Pie de Palo. Geology 29:703–706

Cassata WS, Renne PR, Shuster DL (2009) Argon diffusion in plagioclase and implications for thermochronometry: a case of study from the Bushveld Complex, South Africa. Geochim Cosmochim Acta 73:6600–6612

Cherniak DJ, Watson EB (2000) Pb diffusion in zircon. Chem Geol 172:5–24

Chernicoff CJ, Zappettini EO (2007) La cuenca neopaleozoica de Arizona, sudeste de San Luis, Argentina: prolongación austral de la Cuenca de Paganzo. Rev Asoc Geol Arg 62:321–324

Costa CH, Vita Finzi C (1996) Late Holocene faulting in the southeast Sierras Pampeanas of Argentina. Geology 24:1127–1130

Coughlin TJ, O´Sullivan PB, Kohn BP, Holcombe RJ (1998) Apatite fission-track thermochronology of the Sierras Pampeanas, central western Argentina: implications for the mechanism of plateau uplift in the Andes. Geology 26:999–1002

Criado Roque P, Mombrú C, Moreno J (1981) Sedimentitas Mesozoicas. In: Yrigoyen M (ed) Geología y Recursos Naturales de la Provincia de San Luis. Relatorio 8 Congreso Geológico Argentino, pp 79–96

Dahl PS (1997) A crystal-chemical basis for Pb retention and fission-track annealing systematics in U-bearing minerals, with implications for geochronology. Earth Planet Sci Lett 150:277–290

Dahlquist JA, Alasino PH, Eby NG, Galindo C, Casquet C (2010) Fault controlled Carbonifeours A-type magmatism in the proto-Andean foreland (Sierras Pampeanas, Argentina): Geochemical constraints and petrogenesis. Lithosphere 115:65–81

Dahlquist JA, Basei MAS, Alasino PH, Saavedra J, Baldo EG, da Costa Campos Neto M, Casquet C (2014) The geological setting of Carboniferous magmatism in the proto-Andean margin of Gondwana, Sierras Pampeanas, Argentina, Paper present at the Gondwana 14 conference, Madrid, Spain

Dahlquist JA, Pankhurst RJ, Rapela CW, Basei MAS, Alasino PH, Saavedra J, Baldo EG, Murro JA, da M Costa Campos Neto, (2015) The Capilla del Monte pluton, Sierras de Córdoba, Argentina: the easternmost Early Carboniferous magmatism in the pre-Andean SW Gondwana margin. Int J Earth Sci. doi:10.1007/s00531-015-1249-0

Dávila FM, Carter C (2013) Exhumation history of the Andean broken foreland revisited. Geology 41:443–446

Davis R (1931) A correlated color temperature for illuminants. Bur Stand J Res 7:659

Dodson MH (1973) Closure temperature in cooling geochronological and petrological systems. Contrib Mineral Petr 40:259–274

Enkelmann E, Ridgway KD, Carignano C, Linnemann U (2014) A thermochronometric view into an ancient landscape: tectonic setting, development, and inversion of the Paleozoic eastern Paganzo basin, Argentina. Lithosphere 6:93–107

Fernández Seveso F, Tankard AJ (1995) Tectonics and stratigraphy of the Late Paleozoic Paganzo Basin of western Argentina and its regional implications. In: Tankard AJ, Suárez R, Welsink HJ (eds) Petroleum basins of South America. AAPG Memoir, vol 62, pp 285–301

Foland KA (1994) Argon diffusion in feldspar. In: Parsons I (ed) Feldspars and their reactions. Kluwer, Dordrecht, pp 415–447

Garber JM, Roeske SM, Warren J, Mulcahy SR, McClelland W, Austin LJ, Renne PR, Vujovich GI (2014) Crustal shortening, exhumation, and strain localization in a collisional orogeny: the Bajo Pequeño Shear Zone, Sierra de Pie de Palo, Argentina. Tectonics 33:1277–1303

Geuna SE, Escosteguy LD, Limarino CO (2010) Paleomagnetism of the Carboniferous-Permian Patquía Formation, Paganzo basin, Argentina: implications for the apparent polar wander path for South America and Gondwana during the Late Palaezoic. Geol Acta 8:373–397

González Bonorino F (1950) Algunos problemas geológicas de las Sierras Pampeanas. Rev Asoc Geol Argentina 5:81–110

González Dıaz EF (1981) Geomorfología. In: Yrigoyen M (ed) Geología y Recursos Naturales de la Provincia de San Luis. Relatorio 8 Congreso Geológico Argentino, pp 193–236

Gordillo C, Lencinas A (1979) Sierras Pampeanas de Córdoba y San Luis. In: Turner JC (ed) Segundo Simposio de Geología Regional Argentina. Academia Nacional de Ciencias, pp 577–650

Gulbranson EL, Montañez IP, Schmitz MD, Limarino CO, Isbell JL, Marenssi SA, Crowley JL (2010) High-precision U–Pb calibration of Carboniferous glaciation and climate history, Paganzo Group, NW Argentina. Geol Soc Am Bull 122:1480–1498

Gutscher MA, Spakman W, Bijwaard H, Engdahl ER (2000) Geodynamic of flat subduction: seismicity and tomographic constraints from the Andean margin. Tectonics 19:814–833

Harrison TM (1981) Diffusion of ^{40}Ar in hornblende. Contrib Mineral Petrol 78:324–331

Harrison TM, Heizler MT, Lovera OM, Chen W, Grove M (1994) A chlorine disinfectant for excess argon released from K-feldspar during step heating. Earth Planet Sci Lett 123:95–104

Harrison TM, Célérier J, Aikman AB, Hermann J, Heizler MT (2009) Diffusion of ^{40}Ar in muscovite. Geochim Cosmochim Acta 73:1039–1051

Hilley GE, Coutand I (2010) Links between topography, erosion, rheological heterogeneity, and deformation in contractional settings: insights from the central Andes. Tectonophysics 495:78–92

Hongn F, Ferreira L, Morello O, Rubinstein N, Kirschbaum A, Guidi F, Anesa J (2010) Control estructural sobre el plutón Los Ratones y la mineralización de uranio en la sierra de Fiambalá, Sierras Pampeanas, Catamarca. Rev Asoc Geol Argentina 67:545–561

Introcaso A, Lion A, Ramos VA (1987) La estructura profunda de las Sierras de Córdoba. Rev Asoc Geol Argentina 42:117–178

Jordan TE, Allmendinger RW (1986) The Sierras Pampeanas of Argentina: a modern analogue of Rocky Mountain foreland deformation. Am J Sci 286:737–764

Jordan TE, Isacks BL, Allmendinger RW, Brewer JA, Ramos VA, Ando CJ (1983) Andean tectonics related to geometry of subducting Nazca Plate. Geol Soc Am Bull 94:341–361

Jordan T, Zeitler P, Ramos V, Gleadow A (1989) Thermochronometric data on the development of the basement peneplain in the Sierras Pampeanas. J S Am Earth Sci 2(3):207–222

Kay SM, Abbruzzi JM (1996) Magmatic evidence for Neogene lithospheric evolution of the central Andean "flat-slab" between 30°S and 32°S. Tectonophysics 259:15–28

Kleiman LE, Japas MS (2009) The Choiyoi volcanic province at 34°S–36°S (San Rafael, Mendoza, Argentina): implications for the Late Palaeozoic evolution of the southwestern margin of Gondwana. Tectonophysics 473:283–299

Krol MA, Simpson C (1999) ^{40}Ar/^{39}Ar cooling ages form micas in the eastern Sierras Pampeanas accretionary prism rocks. Geol Soc Am Abstr Prog 31:114–115

Krol MA, Whitmeyer SJ, Simpson C (2000) ^{40}Ar/^{39}Ar dating of ductile shear zones in the Sierras Pampeanas, central Argentina: implications for the Middle Paleozoic tectonic evolution of the paleo-Pacific Gondwana margin. Geol Soc Am Abstr Prog 32:A-506

Lanphere MA, Dalrymple GB (2000) First-principles calibration of ^{38}Ar tracers: Implications for the ages of ^{40}Ar/^{39}Ar fluence monitors. U.S. Geological Survey Professional Paper 1621

Layer PW (2000) Argon-40/argon-39 age of the El'gygytgyn impact event, Chukotka, Russia. Meteorit Planet Sci 35:591–599

Layer PW, Hall CM, York D (1987) The derivation of ^{40}Ar/^{39}Ar age spectra of single grains of hornblende and biotite by laser step heating. Geophys Res Lett 14:757–760

Leal PR, Hartmann LA, Santos JOS, Miró R, Ramos VA (2003) Volcanismo postorogénico en el extremo norte de las Sierras Pampeanas Orientales: nuevos datos geocronológicos y sus implicancias tectónicos. Rev Asoc Geol Arg 58:593–607

Limarino CO, Spalletti LA (2006) Paleogeography of the upper Paleozoic basins of southern South America: an overview. J S Am Earth Sci 22:134–155

Limarino CO, Tripaldi A, Marenssi S, Fauqué L (2006) Tectonic, sea-level, and climatic controls on Late Paleozoic sedimentation in the western basins of Argentina. J S Am Earth Sci 22:205–226

Limarino CO, Spalletti LA, Colombo Piñol F, Ciccioli PL (2013) Dynamics of the Valle Fértil lineament during the late Paleozoic based on petrofacies analysis (Northwest Argentina). B Geofis Teor Appl 1:24

Löbens S, Bense FA, Wemmer K, Dunkl I, Costa CH, Layer C, Siegesmund S (2011) Exhumation and uplift of the Sierras Pampeanas: preliminary implications from K-Ar fault gouge dating and low-T thermochronology in the Sierra de Comechingones (Argentina). Int J Earth Sci 100:671–694

Löbens S, Sobel ER, Bense FA, Wemmer K, Dunkl I, Siegesmund S (2013a) Refined exhumation history of the northern Sierras Pampeanas, Argentina. Tectonics 32:453–472

Löbens S, Bense FA, Dunkl I, Wemmer K, Kley J, Siegesmund S (2013b) Thermochronological constraints of the exhumation and uplift of the Sierra de Pie de Palo, NW Argentina. J S Am Earth Sci 48:209–219

Lovera OM, Richter FM, Harrison TM (1989) The ^{40}Ar/^{39}Ar thermochronometry for slowly cooled samples having a distribution of diffusion domain sizes. J Geophys Res 94:17917–17935

Lovera OM, Richter FM, Harrison TM (1991) Diffusion domains determined by ^{39}Ar release during step heating. J Geophys Res 96:2057–2069

Lovera OM, Heizler MT, Harrison TM (1993) Argon diffusion domains in K-feldspar, II, Kinetic properties of MH-10. Contrib Miner Petrol 113:381–393

Lovera OM, Grove M, Harrison TM (2002) Systematic analysis of K-feldspar ^{40}Ar/3^{9}Ar step heating results: II. Relevance of laboratory argon diffusion properties to nature. Geochim Cosmochim Acta 66:1237–1255

Maffini MN (2015) Estudio petro-estructural, mineralógico y metalogenético de depósitos vetiforms mesotermales (Pb–Zn–Cu–Ag–Au) emplazados en el basamento metamórfico de la Sierra de Comechingones, en proximidad a cuerpos ígneos plutónicos, Sierras Pampeanas Orientales. PhD thesis, Universidad Nacional de Río Cuarto

Maffini MN, Coniglio JE, Demartis M, D'Eramo FJ, Pinotti LP, Bin I, Petrelli HA (2012) Vetas mesotermales de Pb-Zn-Ag-Au emplazadas al este del Batolito Cerro Áspero, Sierra de Comechingones, Córdoba. Serie Correlación Geológica 28:93–106

Mark DF, Kelley SP, Lee MR, Parnell J, Sherlock SC, Brown DJ (2008) Ar-Ar dating of authigenic K-feldspar: quantitative modelling of radiogenic argon-loss through subgrain boundary networks. Geochim Cosmochim Acta 72:2695–2710

Martino RD (2003) Las fajas de deformación dúctil de las Sierras Pampeanas de Córdoba: una reseña general. Rev Asoc Geol Argentina 58:549–571

McDougall I, Harrison TM (1999) Geochronology and thermochronology by the $^{40}Ar/^{39}Ar$ method, 2nd edn. Oxford University Press, New York

McLaren S, Dunlap WJ (2006) Use of $^{40}Ar/^{39}Ar$ K-feldspar thermochronology in basin thermal history reconstruction: an example form the Big Lake Suite granites, Warburton Basin, South Australia. Basin Res 18:189–203

Meert JG, Hall C, Nédélec A, Madison Razanatseheno MO (2001) Cooling of a late-syn orogenic pluton: evidence from laser K-feldspar modelling of the Carion granite, Madagascar. Gondwana Res 4:541–550

Miller H, Söllner F (2005) The Famatina complex (NW Argentina): back-docking of an island arc or terrane accretion? Early Palaeozoic geodynamics at the western Gondwana margin. In: Vaughan APM, Leat PT (eds) Terrane processes at the margin of Gondwana. Geol Soc London Spec. Publ 246: 241–256

Mortimer N, McLaren S, Dunlap WJ (2012) Ar–Ar dating of K-feldspar in low grade metamorphic rocks: example of an exhumed Mesozoic accretionary wedge and forearc, South Island, New Zealand. Tectonics 31:TC3020

Mulcahy SR, Roeske SM, McClelland WC, Jourdan F, Iriondo A, Renne PR, Vervoort JD, Vujovich GI (2011) Structural evolution of a composite middle to lower crustal section: the Sierra de Pie de Palo, northwest Argentina. Tectonics 30:TC1005

Mutti D, Di Marco A, Geuna S (2007) Depósitos polimetálicos en el orógeno famatiniano de las Sierras Pampeanas de San Luis y Córdoba: fluidos, fuentes y modelo de emplazamiento. Rev Asoc Geol Arg 62:44–61

Net LI, Limarino CO (2006) Applying sandstone petrofacies to unravel the Upper Carboniferous evolution of the Paganzo Basin, northwest Argentina. J S Am Earth Sci 22:239–254

Pankhurst RJ, Rapela CW (1998) The proto-Andean margin of Gondwana: an introduction. In: Pankhurst RJ, Rapela CW (eds) The proto-Andean margin of Gondwana. Geol Soc London Spec Pub, vol 142, pp 1–9

Pilger RH (1984) Cenozoic plate kinematics, subduction and magmatism, South American Andes. J Geol Soc Lond 15:59–78

Ramos VA (1988) Late proterozoic-early paleozoic of South America—a collisional history. Episodes 11:168–174

Ramos VA, Dallmeyer RD, Vujovich GI (1998) Time constraints on the Early Palaeozoic docking of the Precordillera, central Argentina. In: Pankhurst RJ, Rapela CW (eds) The proto-Andean margin of Gondwana. Geol Soc London Spec. Publ. vol 142, pp 143–158

Ramos VA, Cristallini EO, Pérez DJ (2002) The Pampean flat-slab of the Central Andes. J S Am Earth Sci 15:59–78

Rapela CW, Pahnkhurst RJ, Casquet C, Baldo E, Saavedra J, Galindo C, Fanning CM (1998) The Pampean orogeny of the southern proto-Andes: evidence for Cambrian continental collision in the Sierras de Córdoba. In: Pankhurst RJ, Rapela CW (eds) The proto-Andean margin of Gondwana. Geol. Soc. London Spec. Publ, vol 142, pp 181–217

Rapela CW, Pahnkhurst RJ, Casquet C, Fanning CM, Baldo E, González-Casado JM, Galindo C, Dahlquist J (2007) The Río de la Plata craton and the assembly of SW Gondwana. Earth-Sci Rev 83:49–82

Richardson T, Gilbert H, Anderson M, Ridgway KD (2012) Seismicity within the actively deforming Eastern Sierras Pampeanas, Argentina. Geophys J Int 188:408–420

Rossello E, Mozetic ME (1999) Caracterización estructural y significado geotectónico de los depocentros cretácicos continentales del centro-oeste argentino. Simposio sobre o Cretáceo do Brasil (Rio Claro) 5:107–113

Samson SD, Alexander EC (1987) Calibration of the interlaboratory $^{40}Ar/^{39}Ar$ dating standard, MMhb1. Chem Geol 66:27–34

Schmidt C, Astini R, Costa C, Gardini C, Kraemer P (1995) Cretaceous rifting, alluvial fan sedimentation, and Neogene inversion, southern Sierras Pampeanas, Argentina. In: Tankard AJ, Suárez R, Welsink HJ (eds) Petroleum basins of South America. AAPG Memoir, vol 62, pp 341–358

Sherlock SC, Lucks T, Kelley SP, Barnicoat A (2005) High spatial resolution $^{40}Ar/^{39}Ar$ laser probe analysis of complex polygenetic K-feldspar overgrowths: a record of sandstone burial and tectonically driven fluid migration. Earth Planet Sci Lett 238:329–341

Siame LL, Sébrier M, Bellier O, Bourlès D, Costa C, Ahumada EA, Gardini CE, Cisneros H (2015) Active basement uplift of Sierra de Pie de Palo (Northwestern Argentina): rates and inception from ^{10}Be cosmogenic nuclide concentrations. Tectonics 34:1129–1153

Siegesmund S, Steenken A, López de Luchi MG, Wemmer K, Hoffmann A, Mosch S (2004) The Las Chacras-Potrerillos batholith (Pampean Ranges, Argentina): structural evidences, emplacement and timing of the intrusion. Int J Earth Sci 93:23–43

Siegesmund S, Steenken A, Martino RD, Wemmer K, López de Luchi MG, Frei R, Presnyakov S, Guereschi A (2010) Time constraints on the tectonic evolution of the Eastern Sierras Pampeanas (Central Argentina). Int J Earth Sci 99:1199–1226

Simpson C, Whitmeyer SJ, De Paor DG, Gromet LP, Miró R, Krol MA, Short H (2001) Sequential ductile to brittle reactivation of major fault zones along the accretionary margin of Gondwana. In: Holdsworth RE, Strachan RA, Magloughlin JF, Knipe RJ (eds) The nature and tectonic significance of fault zone weakening. Geol Soc London Spec Publ, vol 186, pp 233–255

Sims JP, Ireland TR, Camacho A, Lyons P, Pieters PE, Skirrow RG, Stuart-Smith PG, Miró R (1998) U-Pb, Th-Pb and Ar-Ar geochronology from the southern Sierras Pampeanas: implications for the Palaeozoic tectonic evolution of the western Gondwana margin. In: Pankhurst RJ, Rapela CW (eds) The proto-Andean margin of Gondwana. Geol Soc Lond Spec Publ, vol 142, pp 259–281

Spötl C, Kunk MJ, Ramseyer K, Longstaffe FJ (1998) Authigenic potassium feldspar: a tracer for the timing of palaeofluid flow in carbonate rocks, Northern Calcareous Alps, Austria. In: Parnell J (ed) Dating and duration of fluid flow and fluid-rock interaction. Geol Soc Lond Spec Publ, vol 144, pp 107–128

Steenken A, Wemmer K, López de Luchi MG, Siegesmund S, Pawlig S (2004) Crustal provenance and cooling of the basement complexes of the Sierra de San Luis: an insight into the tectonic history of the proto-Andean margin of Gondwana. Gondwana Res 7:1171–1195

Steenken A, Siegesmund S, López de Luchi MG, Frei R, Wemmer K (2006) Neoproterozoic to Early Palaeozoic events in the Sierra de San Luis: implications for the Famatinian geodynamics in the Eastern Sierras Pampeanas (Argentina). J Geol Soc Lond 163:965–982

Steenken A, Wemmer K, Martino RD, López de Luchi MG, Guereschi A, Siegesmund S (2010) Post-Pampean cooling and uplift of the Sierras Pampeanas in the west of Córdoba (Central Argentina). Neues J Geol P A 256: 235–255

Steiger RH, Jaeger E (1977) Subcommission on geochronology: convention on the use of decay constants in geo and cosmochronology. Earth Planet Sci Lett 36:359–362

Streepey MM, Hall CM, van der Pluijm BA (2002) The $^{40}Ar/^{39}Ar$ laser analysis of K-feldspar: constraints on the uplift history of the Grenville Province in Ontario and New York. J Geophys Res 107:2296

Varela R, Basei MAS, González PD, Sato AM, Naipauer M, Campos Neto M, Cingolani CA, Meira VT (2011) Accretion of Grenvillian terranes to the southwestern border of the Río de la Plata craton, western Argentina. Int J Earth Sci 100:243–272

Vujovich GI, Ramos VA (1999) Mapa geotectónico de la República Argentina (1:2500000). Subsecretaría de Minería de la Nación, Servicio Geológico Minero Argentino, Buenos Aires

Wemmer K, Steenken A, Müller S, López de Luchi MG, Siegesmund S (2011) The tectonic significance of K/Ar illite fine-fraction ages from the San Luis formation (Eastern Sierras Pampeanas, Argentina). Int J Earth Sci 100:659–669

Whitmeyer SJ (2008) Dating fault fabrics using modern techniques of 40Ar/39Ar thermochronology: evidence for Paleozoic deformation in the Eastern Sierras Pampeanas, Argentina. J Virtual Explorer. doi:10.3809/jvirtex.2008.00207

Willner AP, Gerdes A, Massonne H-J, Schmidt A, Sudo M, Thomson SN, Vujovich G (2011) The geodynamics of collision of a microplate (Chilenia) in Devonian times deduced by the pressure-temperature-time evolution within part of a collisional belt (Guarguaraz Complex, W-Argentina). Contrib Mineral Petrol 162:303–327

Yáñez G, Ranero GR, von Huene R, Díaz J (2001) Magnetic anomaly interpretation across a segment of the Southern Central Andes (32–34°S): implications on the role of the Juan Fernández Ridge in the tectonic evolution of the margin during the upper Tertiary. J Geophys Res 106:6325–6345

York D, Hall CM, Yanase Y, Hanes JA, Kenyon WJ (1981) 40Ar/39Ar dating of terrestrial minerals with a continuous laser. Geophys Res Lett 8:1136–1138